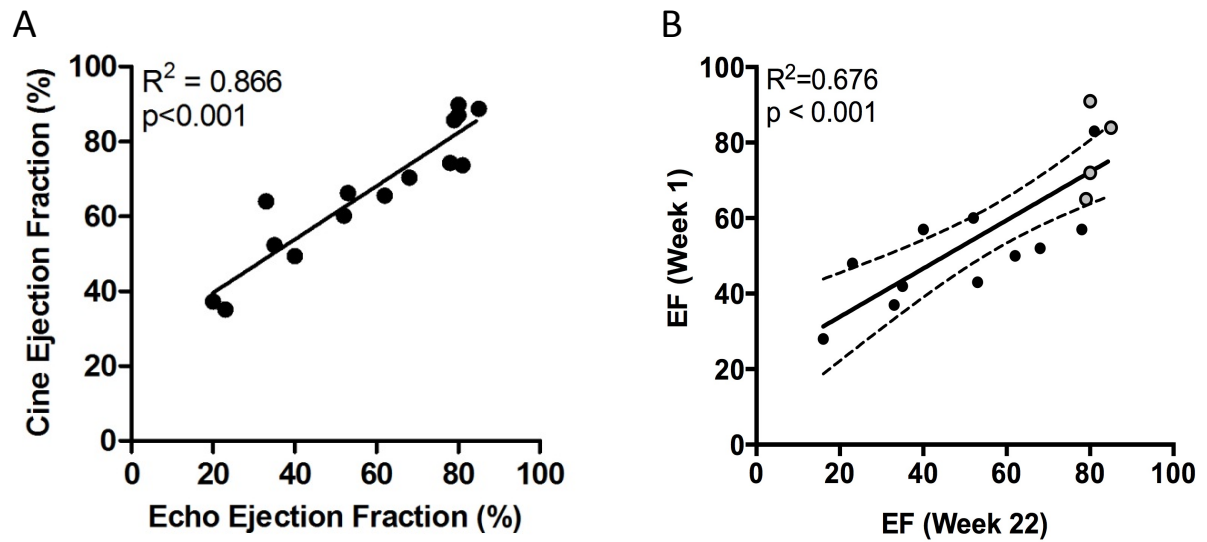
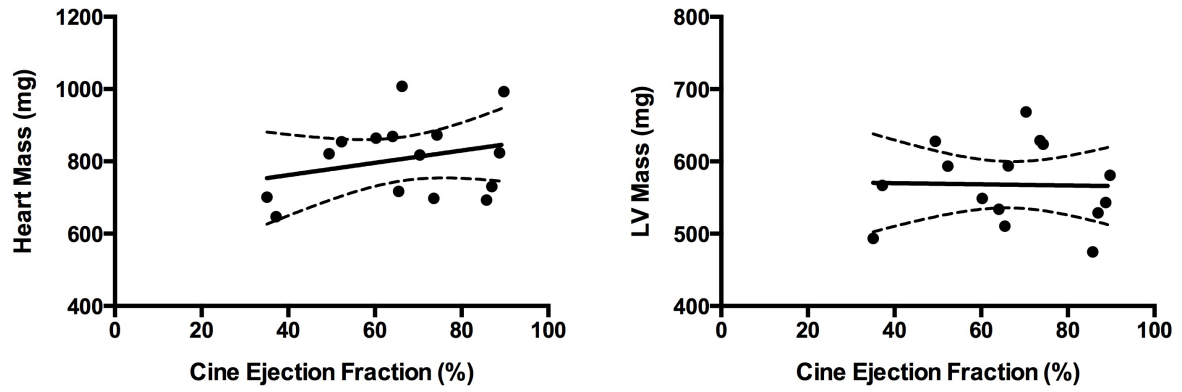


SUPPLEMENTAL MATERIAL

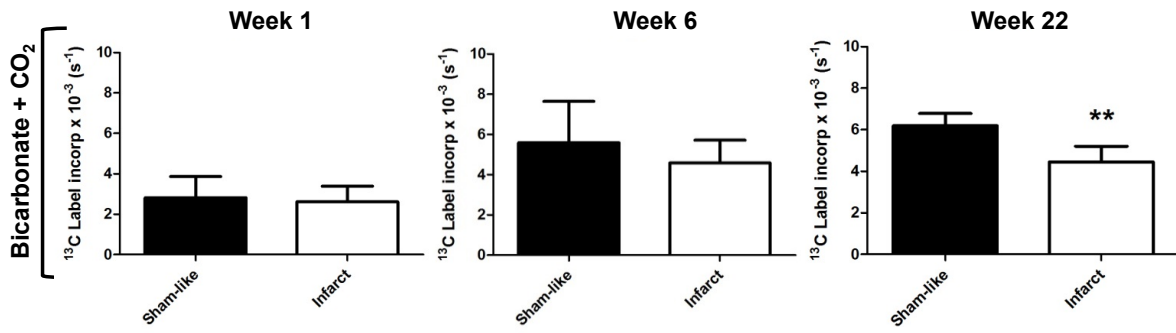
Supplemental Figures



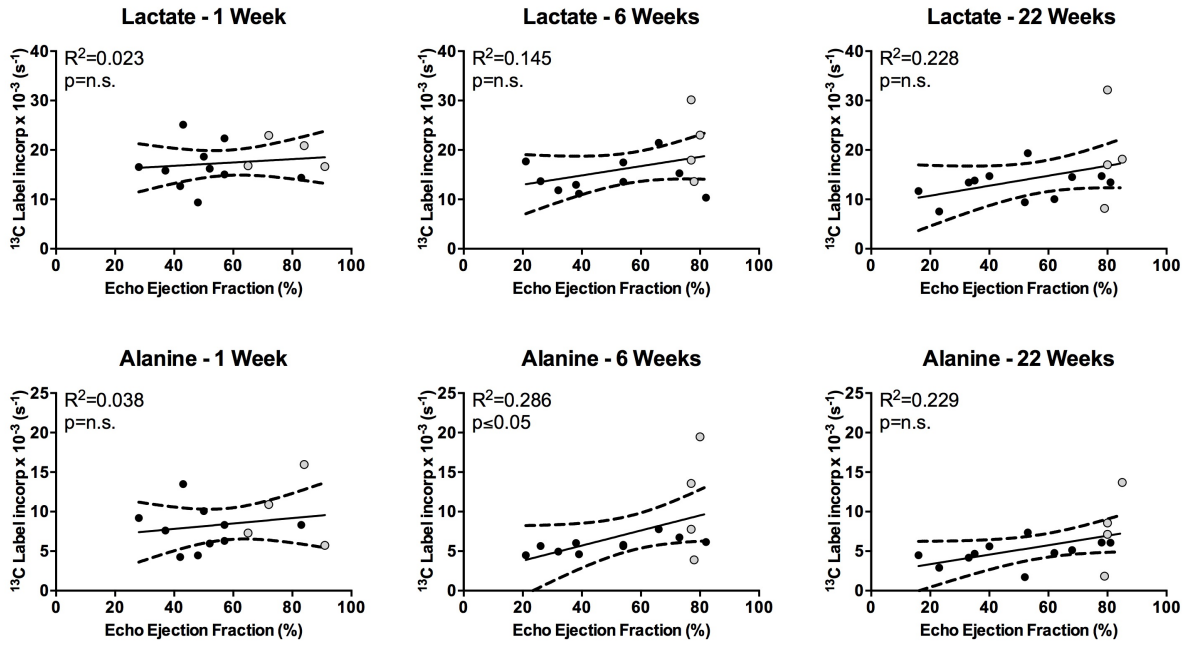
Supplementary Figure 1 – Comparison of Ejection fraction – A) Comparison between cine-MRI and echocardiography – A significant correlation was detected between the ejection fraction measured using cine-MRI and echo. B) A comparison between the ejection fraction at week 1 and week 22. A significant correlation was seen between the two different time points.



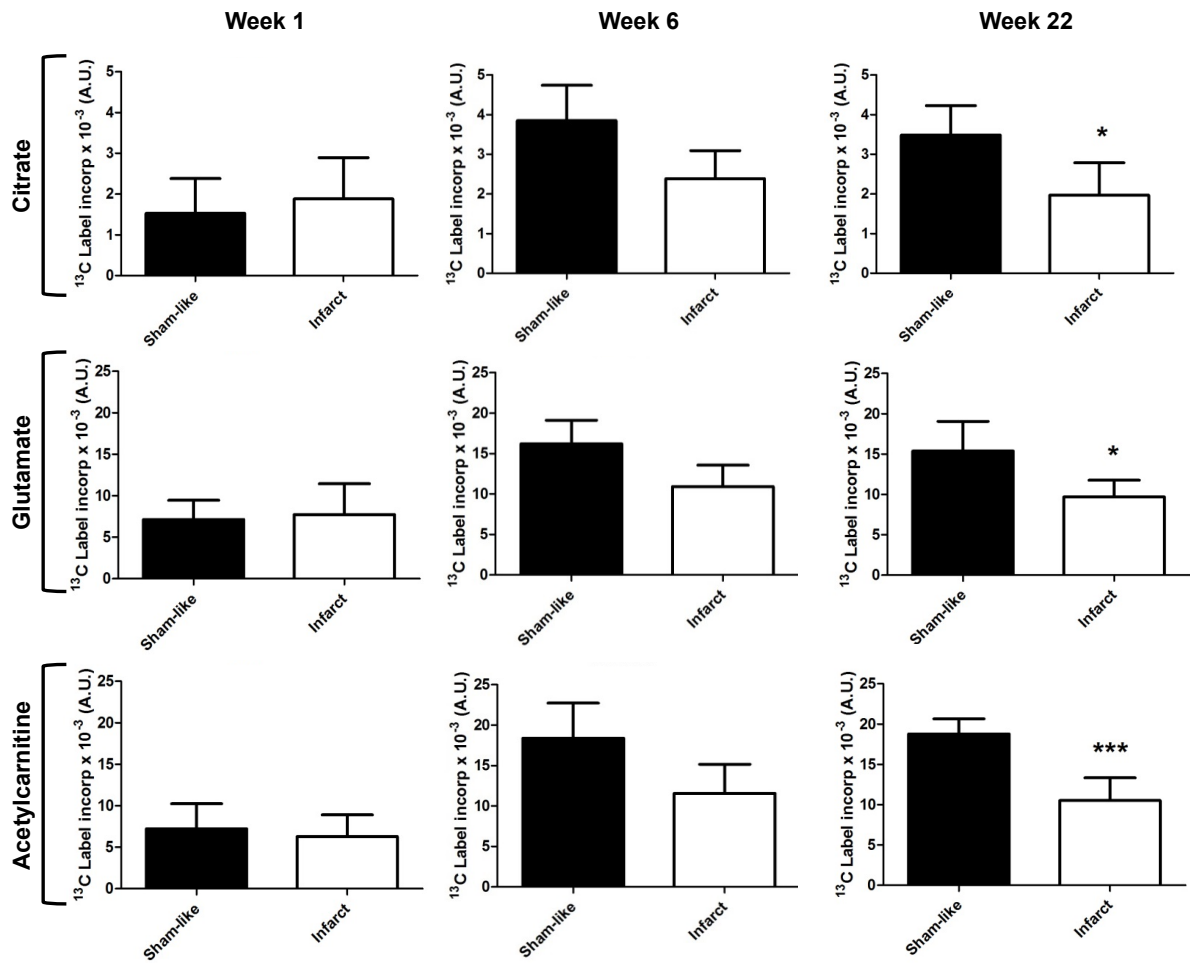
Supplementary Figure 2 – The viable mass of the heart does not correlate with ejection fraction – A) Following sacrifice and tissue collection, the infarct was excised and the rest of the heart was weighed and compared to the *in vivo* ejection fraction. B) The left ventricular mass, minus the scar was assessed *in vivo* by MRI at 22 weeks and compared with the ejection fraction. Both measurements showed that there was no change in either heart mass or LV mass when compared to ejection fraction.



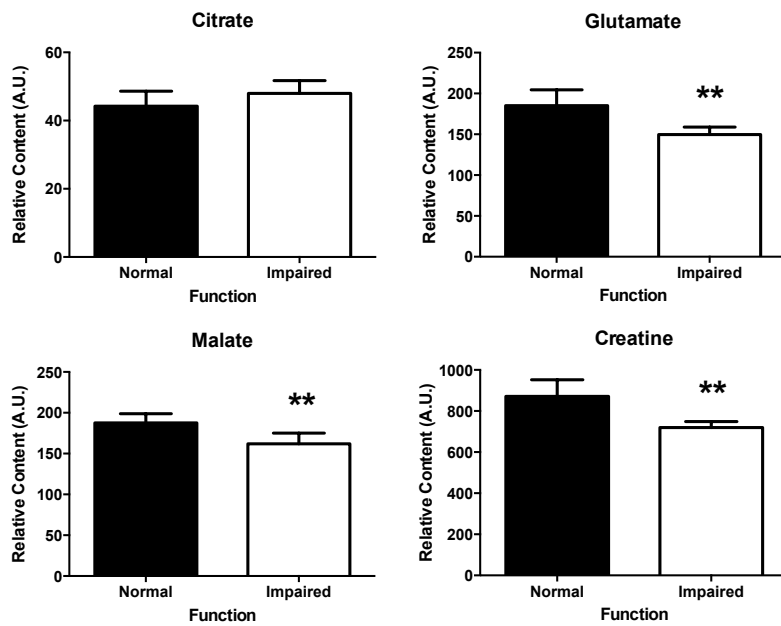
Supplementary Figure 3 – Group analysis of PDH flux – No change is seen in PDH flux until the 22 week time point, where there is a significant reduction in the impaired function group. ** $p < 0.01$. Data is mean with \pm SEM.



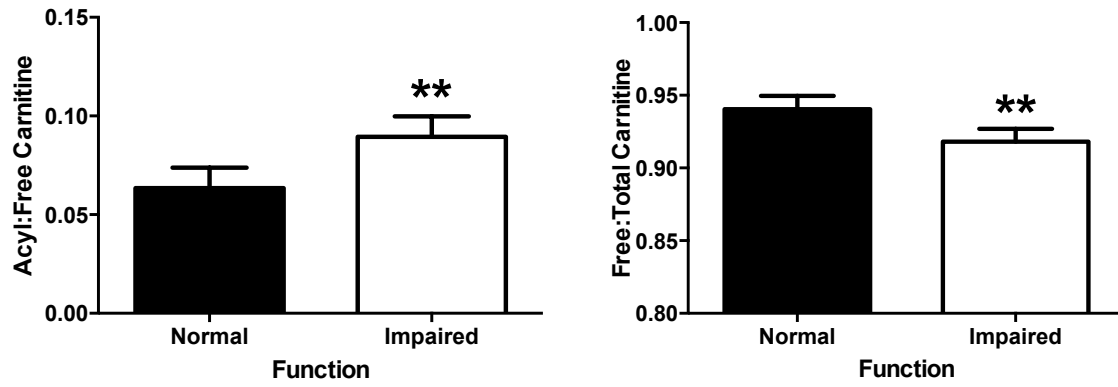
Supplementary Figure 4 – *In vivo* ¹³C label incorporation into lactate and alanine was measured at each time point post-MI – No significant correlation was detected over the range of ejection fractions for lactate but a significant correlation was observed between alanine and ejection fraction at the 6 week time point. (Alanine – 6 weeks and Lactate – 22 weeks were analysed using Spearman Rank Correlation).



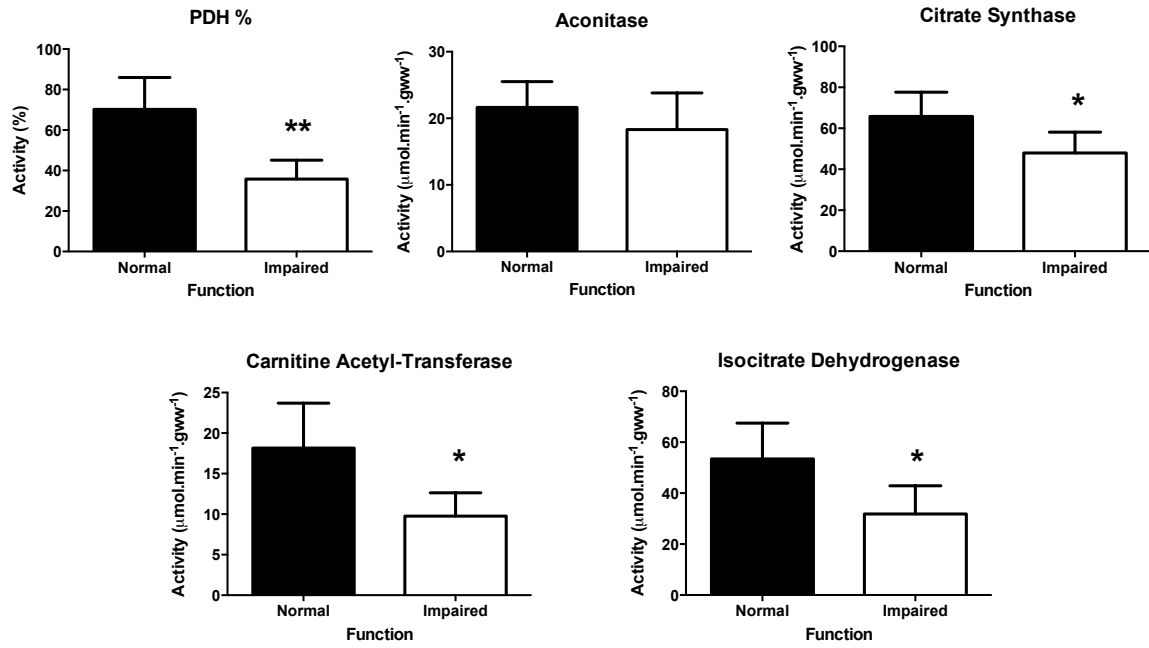
Supplementary Figure 5 – Group analysis of *in vivo* ^{13}C label incorporation into citrate, glutamate and acetylcarnitine was measured at each time point post-MI – By 6 weeks post MI, there was a significant reduction in label incorporation into citrate, glutamate and acetylcarnitine in the impaired function group. This difference was maintained at 22 weeks. * $p < 0.05$ and *** $p < 0.001$. Data is mean with \pm SEM.



Supplementary Figure 6 – Group analysis of *in vitro* analysis of metabolite pool sizes at 22 weeks – No difference in citrate pool size was seen between normal and impaired function animals. Glutamate, malate and creatine were all reduced in the impaired hearts. ** $p < 0.01$. Data is mean with \pm SEM.



Supplementary Figure 7 – Group analysis of *in vitro* carnitine availability at 22 weeks – A significant increase in the acylcarnitine to free carnitine ratio is seen in the impaired function group. Coupled with this, there is a significant reduction in the free carnitine to total carnitine ratio. ** $p < 0.01$. Data is mean with \pm SEM.



Supplementary Figure 8 – Group analysis of *in vitro* analysis of enzyme activity at 22 weeks – A significant decrease in enzyme activity of PDH, citrate synthase, carnitine acetyl-transferase and isocitrate dehydrogenase is seen in the impaired function group. No difference is seen between groups for the activity of aconitase. * $p < 0.05$ ** $p < 0.01$. Data is mean with \pm SEM.

Detailed Methods

Myocardial Infarction:

The left anterior descending (LAD) coronary artery of female Wistar rats (~200g, n =11) was occluded approximately 2 mm from its origin. Rats were anaesthetized with 2.5 % isoflurane in O₂, intubated, and maintained at 80-90 breaths per minute with a tidal volume of 2-3 ml. Thoracotomy was performed in the 4th intercostal space, the pericardium was removed and a 5-0 proline suture was placed under the LAD. The suture was tied around a small piece of PE tubing, occluding the LAD and the chest closed. Animals were subjected to 3,000 seconds (sec) of coronary artery occlusion, the chest was re-opened and the tubing removed to allow reperfusion. Sham-operated animals underwent the same procedure but without coronary ligation (n = 4).

Echocardiography

Animals were lightly anaesthetized with isoflurane and 2D-echocardiography was performed as described.¹ LV short axis images were acquired at the mid-papillary level using a Philips SONOS 5500 system with a 12MHz transducer giving one image every 8.3ms. Three separate acquisitions were made at approximately the same mid-papillary level, and endocardial borders and dimensions were measured, excluding papillary muscles, at end systole and end diastole from three consecutive heart cycles. Images acquired during inspiration were excluded. Ejection fraction (EF = End systolic area/End diastolic area) were calculated from this mid-papillary slice.

MRI measurements of cardiac function

At week 22, post hyperpolarized MRS analysis, cardiac function was assessed using MRI as described previously.¹ The animals remained anesthetized with 1.5% to 2.5% isoflurane in O₂ and positioned supine in a purpose-built, temperature- regulated cradle. ECG electrodes were inserted into the

forepaws and a respiration loop was taped across the chest. The cradle was lowered into a vertical-bore 500 MHz, 11.7 T MR system with a Bruker console and a 52-mm birdcage RF coils (Rapid Biomedical, Würzburg, Germany). ECG and respiration trigger levels were adjusted so that acquisitions were triggered at the same point in the cardiac cycle. Long and short-axis scout images were acquired so that true short-axis images could be planned using a segmented, ECG-triggered fast low-angle shot (FLASH) sequence. The RF coil was then tuned and matched, followed by slice selective shimming. Cine-MR images, consisting of 28–35 frames per heart cycle, were acquired in seven to eight contiguous slices in the short-axis orientation covering the entire heart. The imaging parameters were as follows: field of view (FOV) = 51.2×51.2 mm, matrix size = 256×256 , slice thickness = 1.5 mm giving a voxel size 0.015 mm^3 , echo time (TE)/repetition time (TR) = 1.43/ 4.6 ms, $0.5 \text{ ms}/17.5^\circ$ Gaussian RF excitation pulse, and four averages. The total experimental time, including animal preparation, was approximately 50 min per animal. Heart rate remained stable throughout the procedure. End-diastolic (ED) and end-systolic (ES) frames were selected as those with the largest and smallest cavity volumes, respectively. Epicardial and endocardial borders were outlined using the free-hand drawing function of ImageJ (National Institutes of Health, USA). Measurements from all slices were summed to calculate ED volume (EDV), (SV = EDV - ES volume), ejection fraction (EF = SV/EDV) and cardiac output (CO = SV \times heart rate).

Hyperpolarized ^{13}C MR protocol

Animals received either a [$1\text{-}^{13}\text{C}$]- or [$2\text{-}^{13}\text{C}$]pyruvate scan, 1 hour apart with the order randomised (Sigma-Aldrich, UK). A home-built $^1\text{H}/^{13}\text{C}$ butterfly coil (loop diameter, 2 cm) was placed over the rat chest, localizing signal from the heart. Rats were positioned in a 7 T horizontal bore MR scanner interfaced to an Inova console (Varian Medical Systems). Correct positioning was confirmed by the acquisition of an axial proton FLASH image (TE/TR, 1.17/2.33 ms; matrix size, 64×64 ; FOV, 60×60 mm; slice thickness, 2.5 mm; excitation flip angle, 15°). An ECG-gated shim was used to reduce the proton linewidth to ~ 120 Hz. One millilitre of hyperpolarized pyruvate was injected over 10 s into

the anaesthetised rat. Sixty individual ECG-gated ^{13}C MR pulse-acquire cardiac spectra were acquired over 60 sec after injection (TR, 1 s; excitation flip angle, 5° ; sweep width, 13,593 Hz; acquired points, 2,048; frequency centred on the C1 pyruvate resonance).

MR data analysis

All cardiac ^{13}C spectra were analysed using the AMARES algorithm in the jMRUI software package (Naressi 2001). Spectra were DC offset-corrected based on the last half of acquired points. The peak areas of *in vivo* $[1-^{13}\text{C}]$ pyruvate, $[1-^{13}\text{C}]$ lactate, $[1-^{13}\text{C}]$ alanine, $[^{13}\text{C}]$ carbon dioxide and $[^{13}\text{C}]$ bicarbonate (for $[1-^{13}\text{C}]$ pyruvate), $[1-^{13}\text{C}]$ acetylcarnitine, $[1-^{13}\text{C}]$ citrate and $[5-^{13}\text{C}]$ glutamate (for $[2-^{13}\text{C}]$ pyruvate) at each time point were quantified and used as input data for a kinetic model. The kinetic model developed for the analysis of hyperpolarized $[1-^{13}\text{C}]$ and $[2-^{13}\text{C}]$ pyruvate MRS data is based on a model initially developed by Zierhut *et al*² and further developed by Atherton *et al*³. Firstly the change in labeled pyruvate signal over the 60 s acquisition time was fit to the integrated labeled pyruvate peak area data using equation [1]:

$$[1] \quad M_{pyr}(t) = \begin{cases} \frac{rate_{inj}}{k_{pyr}} \left(1 - e^{-k_{pyr}(t-t_{arrival})} \right) & t_{arrival} \leq t < t_{end} \\ M_{pyr}(t_{end}) e^{-k_{pyr}(t-t_{end})} & t \geq t_{end} \end{cases}$$

In this equation, $M_{pyr}(t)$ represents the $[1-^{13}\text{C}]$ or $[2-^{13}\text{C}]$ pyruvate peak area as a function of time. This equation fits the parameters k_{pyr} , the rate constant for pyruvate signal decay (s^{-1}), $rate_{inj}$, the pyruvate arrival rate (a.u. s^{-1}), $t_{arrival}$, the pyruvate arrival time (s) and t_{end} , the time correlating with the end of the injection (s). These parameters were used in equation [2] along with the dynamic metabolite data to calculate $k_{pyr \rightarrow X}$, the rate of ^{13}C label incorporation into each metabolite pool from pyruvate (s^{-1}) and

k_x , the rate constant for signal decay of each metabolite (s^{-1}) which was assumed to consist of metabolite T_1 decay and signal loss from the 5° RF flip angle pulses. Where t' is $t - t_{\text{delay}}$, and accounts for delay in the circulation of hyperpolarized pyruvate through the cardiac micro-vascular.

$$[2] \quad M_x(t') = \begin{cases} \frac{k_{\text{pyr} \rightarrow x} \text{rate}_{\text{inj}}}{k_{\text{pyr}} - k_x} \left(\frac{1 - e^{-k_x(t' - t'_{\text{arrival}})}}{k_x} - \frac{1 - e^{-k_{\text{pyr}}(t' - t'_{\text{arrival}})}}{k_{\text{pyr}}} \right) & t'_{\text{arrival}} \leq t' < t'_{\text{end}} \\ \frac{M_{\text{pyr}}(t'_{\text{end}}) k_{\text{pyr} \rightarrow x}}{k_{\text{pyr}} - k_x} \left(e^{-k_x(t' - t'_{\text{end}})} - e^{-k_{\text{pyr}}(t' - t'_{\text{end}})} \right) + M_x(t'_{\text{end}}) e^{-k_x(t' - t'_{\text{end}})} & t' \geq t'_{\text{end}} \end{cases}$$

Enzyme Activity analysis

Citrate synthase activity assay

The activity of citrate dehydrogenase was determined spectrophotometrically in a reaction monitoring the increase in absorbance at 412 nm due to the conversion of 5,5'-Dithiobis(2-nitrobenzoic acid) (DTNB) to 2-nitro-5-thiobenzoate (TNB).^{4,5} To a plastic cuvette, add assay buffer [100 μ l; 1 M tris HCl, 1 mmol/L DTNB, neutralized to pH 8.1 with sodium hydroxide and made up to 100 ml in double distilled water], acetyl-CoA [50 μ l; Add 1 ml of ice cold dd H₂O to 10 mg Coenzyme A hydrate, then add 100 μ l 1 M potassium bicarbonate and 2 μ l acetic anhydride, mix and incubate on ice for 600 sec. Add a further 2 μ l acetic anhydride, mix and incubate for another 600 sec. Dilute with 4.416 ml of dd H₂O], 750 μ l dd H₂O and 50 μ l of homogenised sample. The cuvette was incubated in a heat block at 30 °C for 300 sec and used to zero the UV spectrophotometer at 340 nm. 50 μ l of 10 mmol/L oxaloacetate was added, mixed and the increase in absorbance recorded at 340 nm and 30 °C for 240 seconds (using an extinction coefficient for NADH of 6270 mmol/L.cm⁻¹), using UV probe chart reader software (Shimadzu) and a Shimadzu UV-1700 spectrophotometer. Each supernatant was run in duplicate and the average change in absorbance was used to calculate the activity in (nmol/ min/ mg).

Carnitine acetyltransferase activity

The activity of carnitine acetyltransferase was determined spectrophotometrically by the methods of Marquis and Fritz (1965), Pearson *et al* (1974) and Grizard *et al* (1992), in a coupled reaction monitoring the production of NADH.⁶⁻⁸ 10 µl of 30 µmol/L O-Acetyl-L-carnitine hydrochloride (Sigma-Aldrich, UK) was added to assay buffer [840 µl; 100 mmol/L tris base, 10 mmol/L L-malic acid sodium salt, 1.25 mmol/L ethylene glycol tetra-acetic acid (EDTA) dipotassium salt (first three reagents were added to approximately 40 ml of double distilled water and neutralized to pH 7.4 with hydrochloric acid), 0.5 mmol/L β-nicotinamide adenine dinucleotide hydrate (NAD) and 0.125 mmol/L Coenzyme A hydrate, 4 µM rotenone, 35 U citrate synthase (porcine heart) and 275 U malate dehydrogenase (pigeon heart), made up to 50 ml in double distilled water] and incubated for 600 sec at 37 °C. 150 µl of homogenised sample was added to the assay buffer/acetylcarnitine and incubated for a further 30 seconds at 37 °C. Absorbance was then recorded at 340 nm and 37 °C for 100 seconds (using an extinction coefficient for NADH of 6270 mmol/L.cm), using UV probe chart reader software (Shimadzu) and a Shimadzu UV-1700 spectrophotometer. Each supernatant was run in duplicate and the average change in absorbance was used to calculate the activity in (nmol/ min/ mg).

Aconitase activity

The activity of aconitase was determined spectrophotometrically in a reaction monitoring the decrease in absorbance at 240 nm due to the conversion of *cis*-aconitate to isocitric acid.⁵ Using quartz cuvettes, 890 µl of 50 mmol/L tris hydrochloride (neutralized to pH 7.5 using sodium hydroxide) was used to zero the UV spectrophotometer at 240 nm. The addition of 10 µl *cis*-aconitate, results in a small increase in absorbance for 60 sec, before stabilizing. 100 µl of homogenised sample was added, mixed and decrease in absorbance recorded at 240 nm and 37 °C for 100 seconds (using an extinction coefficient for *cis*-aconitate of 3600 mmol/L.cm), using UV probe chart reader software (Shimadzu) and a Shimadzu UV-1700 spectrophotometer. Each supernatant was run in duplicate and the average change in absorbance was used to calculate the activity in (nmol/ min/ mg).

Isocitrate dehydrogenase activity assay

The activity of isocitrate dehydrogenase was determined spectrophotometrically in a reaction monitoring the increase in absorbance at 340 nm due to the conversion of NAD to NADH.⁵ Using plastic cuvettes, 900 µl of assay buffer was used to zero the UV spectrophotometer at 340 nm [Assay buffer: phosphate buffer [33.3 mmol/L dipotassium phosphate, 22.2 mmol/L potassium phosphate were added to approximately 30 ml of double distilled water and neutralized to pH 7 with potassium hydroxide], 2.8 mmol/L isocitrate, 20 mmol/L citrate, 19.7 mmol/L magnesium chloride, 5 mmol/L adenosine diphosphate, 2.2 mmol/L β-nicotinamide adenine dinucleotide hydrate, 0.05 % bovine serum albumin and 0.18 % triton X-100), and made up to 50 ml in double distilled water]. The assay buffer was incubated in a heat block at 30 °C for 120 sec. 100 µl of sample was added, mixed and the increase in absorbance recorded at 340 nm and 37 °C for 60 seconds (using an extinction coefficient for NADH of 6270 mmol/L.cm⁻¹), using UV probe chart reader software (Shimadzu) and a Shimadzu UV-1700 spectrophotometer. Each supernatant was run in duplicate and the average change in absorbance was used to calculate the activity in (nmol/ min/ mg).

PDH Activity

The activity of the active and total fractions of PDH (PDHa and PDHt) were determined spectrophotometrically by the method of Seymour and Chatham⁹. The PDH assay required the preparation of cardiac tissue with one of two homogenisation buffers for either PDHa or PDHt measurement. PDHa was assessed when PDH was extracted under conditions in which both PDP and PDK were inhibited [25 mmol/L N-2-hydroxyethylpiperazine-N'-2-ethanesulfonic acid (HEPES), 25 mmol/L KH₂PO₄, 25 mmol/L KF, 1 mmol/L DCA, 3 mmol/L ethylenediaminetetraacetic acid, 1 mmol/L adenosine diphosphate (ADP), 1 mmol/L dithiothreitol, 0.05 mmol/L leupeptin, 1% Triton X-100; pH 7.2]. PDHt was assessed under conditions in which PDP was stimulated by Mg²⁺ and PDK was inhibited by DCA and ADP (75 mmol/L HEPES, 5 mmol/L DCA, 5 mmol/L MgCl₂, 1 mmol/L ADP, 1 mmol/L dithiothreitol, 0.05 mmol/L leupeptin, 1% Triton X-100; pH 7.2). Frozen cardiac

tissue was powdered and 0.2 g was homogenised in 1 mL of the appropriate homogenisation buffer using a polytron (30 s). The sample was snap frozen in liquid nitrogen, thawed and rehomogenised three times. The sample was centrifuged (1000 x g, 420 sec) and the supernatant was removed for analysis. Assay buffer [950 mL; 50 mmol/L HEPES, 1 mmol/L MgCl₂, 0.08 mmol/L ethyleneglycol-bis(β-aminoethyl)-N,N,N',N'-tetraacetic acid, 1 mmol/L dithiothreitol, 4 mmol/L rotenone, 1.7 mmol/L nicotinamide adenine dinucleotide (NAD), 0.1 mmol/L coenzyme A, 0.2 mmol/L thiamine pyrophosphate HCl, 16.7 mmol/L lactate; pH 7.2] was incubated with 2 mL lactate dehydrogenase (LDH) at 30 °C for 300 sec. PDH activity was determined by adding and mixing a 25 mL aliquot of either PDHa or PDHt extract with the assay buffer and immediately following the reaction at 340 nm using the kinetic program on a spectrophotometer (120 sec for both PDHa and PDHt samples). The rate of NADH production over the first 30 sec was used to determine the activity in units of mmol/min/ g wet weight.

NMR metabolomic analysis

Metabolites were extracted from heart tissue using methanol/chloroform/water.¹⁰ Frozen tissue (~100 mg) was placed in methanol-chloroform (2:1, 600 µl) and homogenised. Samples were then sonicated for 5 min before chloroform-water (1:1) was added (200 µl of each). Samples were centrifuged (13,500 rpm, 20 min), and the aqueous layer was pipetted off and dried overnight in an evacuated centrifuge (Eppendorf, Hamburg, Germany).

The dried extracts were rehydrated in 600 µl of D₂O and buffered in 0.24 M sodium phosphate (pH 7.0) containing 1 mM sodium-3-(tri-methylsilyl)-2,2,3,3-tetradeuteriopropionate (TSP; Cambridge Isotope Laboratories, Andover, MA) as an internal standard. The samples were analysed using an Avance II+ spectrometer operating at 500 MHz for the ¹H frequency (Bruker) equipped with a 5 mm Broadband TXI Automatic Tuning and Matching (ATMA) probe. Spectra were collected using a solvent suppression pulse sequence based on a 1D- nuclear Overhauser effect spectroscopy pulse sequence to saturate the residual [¹H] water proton signal (relaxation delay = 2 s, t_1 = 3 µs, mixing time

= 150 ms, solvent pre-saturation applied during the relaxation time and the mixing time). One hundred twenty-eight transients were collected into 16 K data points over a spectral width of 12 ppm at 37 °C. NMR spectra were processed using an ACD SpecManager 1D NMR processor (version 8; ACD, Toronto, Canada). Spectra were Fourier transformed after multiplication by a line broadening of 1 Hz and referenced to TSP at 0.0 ppm. Spectra were phased and baseline corrected manually. Each spectrum was integrated using 0.04 ppm integral regions between 0.5–4.5 and 4.7–9.5 ppm. Each 0.04 ppm region was treated as an independent variable during analysis. To account for any difference in concentration between samples, each spectral region was normalised to total integral area. Resonances in the NMR spectra were assigned with reference to the literature or through the analysis of standard compounds.

Acylcarnitine : free carnitine assay

Cardiac tissue (50 mg) was pulverised and extracted using methanol/chloroform/water as described above. The dried organic and aqueous fractions were butylated with hydrogen chloride-1-butanol (50 µl, 3 M) at 60°C for 15 min, dried under nitrogen and reconstituted in 200 µl acetonitrile containing 8 isotopically-labelled carnitine derivatives of known concentration as an internal standard (Cambridge Isotope Laboratories Ltd., USA). Samples were injected (10 µl) into a Quattro Premiere XE Triple Quadrupolar Mass Spectrometer (Waters Ltd, UK) coupled with an ESI source in positive ion mode. The source temperature was 110°C and the capillary voltage used was 3.5 kV. The acylcarnitines were analysed by multiple reaction monitoring (MRM) in positive ion mode. The cone voltage was 35 V, collision energy was 15 eV and the MRM transitions used incorporated a common loss of $m/z = +85$ corresponding to loss of the carnitine head group. Samples were introduced by direct infusion (analysis time = 2 min, flow rate = 10 µl/min, increased linearly by 100 µl/min during the final min, mobile phase = 1:1 acetonitrile: isopropanol + 0.2% formic acid). Data were processed using the Neolynx software package (Waters Ltd, UK).

References

1. Stuckey DJ, Carr CA, Tyler DJ, Clarke K. Cine-MRI versus two-dimensional echocardiography to measure in vivo left ventricular function in rat heart. *NMR Biomed.* 2008;21:765–772.
2. Zierhut ML, Yen Y-FF, Chen AP, Bok R, Albers MJ, Zhang V, Tropp J, Park I, Vigneron DB, Kurhanewicz J, Hurd RE, Nelson SJ. Kinetic modeling of hyperpolarized ¹³C1-pyruvate metabolism in normal rats and TRAMP mice. *J Magn Reson.* 2010;202:85–92.
3. Atherton HJ, Schroeder MA, Dodd MS, Heather LC, Carter EE, Cochlin LE, Nagel S, Sibson NR, Radda GK, Clarke K, Tyler DJ. Validation of the in vivo assessment of pyruvate dehydrogenase activity using hyperpolarised (¹³C MRS. *NMR Biomed.* 2011;24:201–8.
4. Heather LC, Cole MA, Lygate CA, Evans RD, Stuckey DJ, Murray AJ, Neubauer S, Clarke K. Fatty acid transporter levels and palmitate oxidation rate correlate with ejection fraction in the infarcted rat heart. *Cardiovasc Res.* 2006;72:430–7.
5. Darley-Usmar V, Rickwood D, Wilson M. Mitochondria, a practical approach. IRL Press, Oxford; 1987.
6. Marquis NR, Fritz IB. The Distribution of Carnitine, Acetylcarnitine, and Carnitine Acetyltransferase in Rat Tissues. *J Biol Chem.* 1965;240:2193–6.
7. Pearson DJ, Tubbs PK, Chase FA. Carnitine and acylcarnitine. In: Bergmeyer HU, editor. *Methods of Enzymatic Analysis.* Weinheim, New York: Verlag Chemie, Academic Press; 1974. p. 1758–1771.
8. Grizard G, Lombard-Vignon N, Boucher D. Changes in carnitine and acetylcarnitine in human semen during cryopreservation. *Hum Reprod.* 1992;7:1245–1248.
9. Seymour AM, Chatham JC. The effects of hypertrophy and diabetes on cardiac pyruvate dehydrogenase activity. *J Mol Cell Cardiol.* 1997;29:2771–2778.
10. Atherton HJ, Gulston MK, Bailey NJ, Cheng K-K, Zhang W, Clarke K, Griffin JL. Metabolomics of the interaction between PPAR-alpha and age in the PPAR-alpha-null mouse. *Mol Sys Biol.* 2009;5:259.